

# Synthesis and characterization of $[\text{Ru}(\text{NO})(\text{bpp})\text{Cl} \cdot 2\text{H}_2\text{O}]$ [bpp = *N,N'*-bis(2-pyridinecarboxamide)-1,3-propane dianion] and $[\text{Ru}(\text{NO})(\text{bpe})\text{Cl} \cdot 2\text{H}_2\text{O}]$ [bpe = *N,N'*-bis(2-pyridinecarboxamide)-1,2-ethane dianion]

Carol F. Fortney \*, Steven J. Geib, Fu-tyan Lin, Rex E. Shepherd

*Department of Chemistry, University of Pittsburgh, Pittsburgh, PA 15260, USA*

Received 20 August 2004; accepted 17 September 2004

Available online 29 December 2004

This paper is dedicated to the memory of my advisor and our friend, Professor Rex E. Shepherd, a gifted educator, a respected chemist and a good kind man who did what he believed was right

## Abstract

Two ruthenium nitrosyl bis-pyridyl/biscarboxamido compounds,  $[\text{Ru}(\text{NO})(\text{bpp})\text{Cl} \cdot 2\text{H}_2\text{O}]$  [bpp = *N,N'*-bis(2-pyridinecarboxamide)-1,3-propane dianion] and  $[\text{Ru}(\text{NO})(\text{bpe})\text{Cl} \cdot 2\text{H}_2\text{O}]$  [bpe = *N,N'*-(bis-2-pyridinecarboxamide)-1,2-ethane dianion] have been characterized by  $^1\text{H}$  NMR,  $^{13}\text{C}\{^1\text{H}\}$  NMR, and IR spectroscopies, electrospray ionization mass spectrometry, and X-ray crystallography.

© 2004 Elsevier B.V. All rights reserved.

**Keywords:** Carboxamido ligands;  $\{\text{RuNO}\}^6$ ; Ruthenium nitrosyl; Linear nitrosyl; Split NO

## 1. Introduction

The nitrosyl group's abilities to bind to transition metals in a linear or a bent fashion [1–9], to behave as  $\text{NO}^+$  or  $\text{NO}^-$  [10–12] and to influence, as well as be influenced by, other ligands in the coordination environment [13–21] have been of interest to coordination chemists and theoretical chemists for decades [22–24]. Catalytic applications [25–32] of transition metal nitrosyl compounds are of current interest to organometallic and organic chemists. The recent surge of investigations into the behavior of transition metal nitrosyl compounds by biologists and inorganic biochemists is lar-

gely due to the Nobel Prize winning discovery [33–36] that endothelium-derived relaxing factor is actually nitric oxide and to the realization that nitric oxide is implicated in a multitude of physiological and pathophysiological functions. Photolytic activity, exhibited by some transition metal nitrosyl compounds [37–41], combines with nitric oxide's various biological functions to suggest a myriad of applications related to photodynamic therapy [38,42–54]. As a result of these diverse and important applications many books [10,36,55–65], reviews [1–3,29,34,66–69] and special topic papers [70,71], are devoted to transition metal nitrosyl chemistry. Professor Shepherd's contributions to the transition metal nitrosyl chemical literature include the study of  $[\text{Ru}^{\text{II}}(\text{NO}^+)]^{3+}$  and  $[\text{Ru}^{\text{II}}(\text{NO}^+)\text{Cl}]^{2+}$  coordinated to *N*-(hydroxyethyl)ethylenediamine triacetate ( $\text{hedta}^{3-}$ ) [72,73], bipyridine [74,75], dipyridylamine [76,77], imidazole

\* Corresponding author. Tel.: +1 412 624 1219; fax: +1 412 624 8611.

E-mail address: [cfst5@pitt.edu](mailto:cfst5@pitt.edu) (C.F. Fortney).

donors [78], peptide ligands  $[\text{Ru}(\text{NO})\text{Cl}_3(\text{gly-gly-his})]^{2-}$  (gly-gly-his = diglycylhistidine) and  $[\text{Ru}(\text{NO})\text{Cl}_3(\text{gly-gly-gly})]^{2-}$  (gly-gly-gly = triglycine) [79], the  $\pi$ -donating macrocycle dioxocyclam [80] (dioxocyclam = 1,4,8,11-tetraazacyclotetradecane-5,7-dione), methylated biimidazole [81] donors in  $[\text{Ru}(\text{NO})\text{Cl}(2,2'\text{-bis}(4,5\text{-dimethylimidazole}_2))_2]^{2+}$  with the antitumor agent bleomycin [82], the study of *cis*- $[\text{Ru}(\text{NO})\text{Cl}(\text{bpy})_2]^{2+}$  by ESI-MS [74], and the synthesis and characterization of  $[\text{Ru}(\text{NO})(\text{bpb})\text{Cl}]$  (bpb = *N,N'*-bis(2-pyridinecarboxamide)-1,3-benzene dianion) [83]. Following a brief discussion of the development of our current research, this paper will describe the synthesis, crystal structures and NMR characterization of two  $\{\text{RuNO}\}^6$  compounds  $[\text{Ru}(\text{NO})(\text{bpp})\text{Cl}]$  (bpp = *N,N'*-bis(2-pyridinecarboxamide)-1,3-propane dianion) and  $[\text{Ru}(\text{NO})(\text{bpe})\text{Cl}]$  (bpe = *N,N*-bis(2-pyridinecarboxamide)-1,2-ethane dianion) which are currently under investigation for photolytic activity.

It is well known that the nitrosyl moiety, whether it is bound as  $\text{NO}^+$ ,  $\text{NO}^\bullet$ , or  $\text{NO}^-$ , is sensitive to the nature of the central metal and to the coordination environment [13,21,84,85] and that the nitrosyl group exerts an influence on the reactivity of other ligands [1,71,85–88]. However, the factors that control nitrosyl behavior are incompletely understood. Nonetheless, trends are beginning to emerge from the literature. The following discussion shows how the Shepherd group helped elucidate some of those trends and applied them in efforts to design ruthenium nitrosyl compounds predisposed to photolytic dissociation of nitric oxide.

The investigation of ruthenium nitrosyl polyaminopolycarboxylates, including  $[\text{Ru}^{\text{II}}(\text{NO}^+)(\text{hedta}^{3-})]$  provided the first comparison of separate  $\text{Ru}^{\text{II}}\text{NO}^+$ ,  $\text{Ru}^{\text{II}}\text{NO}^\bullet$ , and  $\text{Ru}^{\text{II}}\text{NO}^-$  complexes with a constant secondary ligand field and with a constant oxidation state for the central metal [73]. The thorough investigation of the  $[\text{RuNO}]^{3+}$  complex of bleomycin illustrated that ruthenium nitrosyl agents can be tuned for cell selectivity and revealed that bleomycin's coordination structure depends on the metal's *d*<sup>n</sup> count as well as on the  $\pi$ -acceptor nature and the hydrogen bonding capacity of  $\text{NO}^+$  or its replacement [74,82]. Studies of the different structural isomers [72] of  $[\text{Ru}^{\text{II}}(\text{NO}^+)(\text{hedta})(\text{H}_2\text{O})]$  illustrated that two nitrogen  $\pi$ -donating ligands *cis* to the nitrosyl group push electron density onto the nitrosyl moiety. Increased electron density on the nitrosyl group is evidenced by a decrease in the NO stretching frequency, an effect which has been correlated with a propensity to lose NO by photolysis [74,83,89–91]. Because amido groups also facilitate cell transport [92–97], peptides such as triglycine (gly-gly-gly) and diglycylhistidine (gly-gly-his) were investigated as amido donor ligands [79]. One conclusion from the peptide investigations was that, even though peptides are desirable ligands that

can be tailored to target specific cell types, their failure to chelate fully under physiological conditions diminishes their potential as ligands for NO transport. If peptides are to be used as transporter ligands, they may have to be connected to synthetic chelates at the Ru(NO) center via biocompatible linkers.

Since multiple coordination to peptides was found to be disfavored below pH 7, the viability of the dioxocyclam ligand [80] was investigated. The hypothesis was that the macrocyclic dioxocyclam ligand would enforce the desired bis-amine/bis-amide chelation. The  $[\text{Ru}(\text{NO})(\text{dioxocyclam})\text{Cl}]$  compound induced lower  $\bar{\nu}_{\text{NO}}$  (1845  $\text{cm}^{-1}$ ) than did the tetra-amino  $[\text{Ru}(\text{NO})(\text{cyclam})]^{2+}$  ( $\bar{\nu}_{\text{NO}} = 1875 \text{ cm}^{-1}$ )<sup>39</sup> (cyclam = 1,4,8,11-tetraazacyclotetradecane), an effect that illustrates the significant shift of electron density to NO by the amido groups in dioxocyclam. The intent was to derivatize dioxocyclam at the methylene carbon between the two carbonyl groups with solubilizing and recognition assisting side chains; however, other strategies were adopted because the dioxocyclam ligand is too costly for use on a large scale. From results obtained in the ESI-MS investigation of *cis*- $[\text{Ru}(\text{NO})\text{Cl}(\text{bpy})_2]^{2+}$  it was concluded that,  $\pi$ -acceptor ligands, by competing with  $\text{NO}^+$  for electron density, weaken the Ru–NO bond, and assist the thermal and gas phase dissociation of  $\text{NO}^\bullet$ . On the other hand  $\pi$ -donor ligands inhibit thermal and gas phase reactions by strengthening backbonding from  $\text{Ru}^{\text{II}}$  to NO [74]. The opposite applies to photolytic loss of  $\text{NO}^\bullet$ ;  $\pi$ -donor ligands facilitate photolytic loss of  $\text{NO}^\bullet$  while  $\pi$ -acceptor ligands inhibit photolytic loss of  $\text{NO}^\bullet$ .  $\pi$ -acceptor ligands, such as aromatic *N*-heterocyclic ligands, inhibit photolytic loss of  $\text{NO}^\bullet$  from ruthenium nitrosyl complexes because they exhibit MLCT to the *N*-heterocyclic  $\pi$ -acceptor and ligand field excitations which are at lower energy than the MLCT-to- $\text{NO}^+$  state [66,74,89,90].

Some observations from the studies described illustrate the rationale behind our selection of ligands and the use of ruthenium as the central metal. Because ruthenium complexes are known to accumulate in tumors [36,98–103] and because the strength of the Ru–NO bond [85] increases the probability that the complex will survive under physiological conditions, ruthenium is the transition metal of choice for nitrosyl compounds designed for photodynamic therapy [90]. Nitrosyl photolability may be controlled by altering the  $\pi$ -donor/ $\pi$ -acceptor character of the ligand set. As one of the best  $\pi$ -donating groups, a deprotonated amido functionality should activate the nitrosyl moiety to photolabilization [90] by pushing electron density onto the nitrosyl group. The amido group's propensity toward water solubility and biocompatibility make chelated amido donors excellent ligands for transporting the ruthenium nitrosyl moiety through biological environments [92–97]. Our

current focus is on developing ruthenium nitrosyl complexes bearing tetradentate, bis-pyridyl/bis-amido ligands, bis-pyridyl/bis-phenolato ligands and mixed amido/phenolato ligands. The pyridyl ligands should help force chelation [90,92,96,104,105] while the strong  $\pi$ -donating bis-amido/bis-phenolato donors have the dual purpose of activating the  $\text{Ru}^{\text{II}}(\text{NO}^+)$  moiety toward photolysis, then stabilizing the  $\text{Ru}^{\text{III}}$ -solvent complex that remains after photolysis [84,90,106–109]. Although the compounds described here were designed to examine the possibility of tuning nitrosyl photolability by modifications of the ligand set in the equatorial plane, we are also investigating the influence of bis pyridyl/bisamido, bispyridyl/bisphenolato and mixed bispyridyl/bisphenolato ligands in a position *trans* to the nitrosyl group. It is well known that ligands *trans* to the nitrosyl group influence the behavior of the NO group by direct interaction with the  $\pi^*$  orbitals of the NO group through the metal center [13,19,66,110–114].

With the above principles in mind we synthesized and characterized the  $\{\text{RuNO}\}^6$  compound  $[\text{Ru}(\text{NO})(\text{bpb})\text{Cl}]$  [83,110] (bpb = *N,N'*-bis(2-pyridinecarboxamide)-1,2-benzene) [104,115,116] by ESI-MS and NMR ( $^1\text{H}$ ,  $^{13}\text{C}$ , HH COSY, HMQC and HMBC) spectroscopy. Publication was delayed due to Professor Shepherd's lengthy illness and unexpected passing. After our paper was submitted, the synthesis, crystal structure and photochemistry of  $[\text{Ru}(\text{NO})(\text{bpb})\text{Cl}]$  were reported by the Mascharak group [89]. The crystal structure reveals a linear Ru–N–O moiety (172.37(14)°), as we expected for a  $\{\text{RuNO}\}^6$  compound [89]. Our IR data ( $\nu_{\text{NO}} = 1867 \text{ cm}^{-1}$ ) is in excellent agreement with theirs and is within the range characteristic of similar linear Ru–N–O complexes [41,42].

This paper discusses the next compounds in a series of Ru(NO) bispyridylbiscarboxamido compounds we are investigating,  $[\text{Ru}(\text{NO})(\text{bpe})\text{Cl} \cdot 2\text{H}_2\text{O}]$  (**3**) (bpe = *N,N'*-bis(2-pyridinecarboxamide)-1,2-ethane dianion) and  $[\text{Ru}(\text{NO})(\text{bpp})\text{Cl} \cdot 2\text{H}_2\text{O}]$  (**5**) (bpp = *N,N'*-bis(2-pyridinecarboxamide)-1,3-propane dianion).

## 2. Experimental

### 2.1. Materials and measurements

$[\text{RuCl}_3 \cdot x\text{H}_2\text{O}]$ ,  $\text{NaNO}_2$ , picolinic acid, 1,2-diaminopropane, 1,2-diaminoethane, pyridine, triphenylphosphite, chloroform and ethanol were obtained from Aldrich and used without further purification.

### 2.2. Instrumentation

$^1\text{H}$ ,  $^{13}\text{C}\{^1\text{H}\}$  NMR, HMQC, and HMBC spectra were obtained on a Bruker AVANCE DRX 500 digital NMR spectrometer. Infrared spectra of KBr or KCl

pellets were obtained on Perkin–Elmer BX FT-IR spectrometer. Mass spectrometry was carried out on a Waters Q-TOF API US instrument using electrospray ionization or on a 571A HP GC–MS instrument.

### 2.3. Syntheses

Trichloronitrosylruthenium (**1**) was prepared using a modification of the procedure of Fletcher et al. [117]  $[\text{RuCl}_3 \cdot x\text{H}_2\text{O}]$  (207.43 g/mol, 2.00 g, 0.0096 mol, 1 equiv.) was dissolved in HCl (1 M, 15.0–18.0 ml, >1 equiv.) and heated to 100 °C in an oil bath. At 100 °C, an aqueous solution of  $\text{NaNO}_2$  (68.9 g/mol, 1.99 g, 3 equiv.) was added dropwise over 1 h. The dark red/black solution began to turn purple as  $\text{NO}_2$  was released. After 1 h the water was removed from the reaction mixture under vacuum (rotary evaporator, 90 °C). The remaining dark purple solid was dissolved in ethanol to separate **1** from NaCl formed in the reaction. NaCl was removed via vacuum filtration. Ethanol was removed under vacuum (rotary evaporator, 65–70 °C). The extremely hygroscopic purple solid was stored in a desiccator with Drierite.

*N,N'*-bis(2-pyridine carboxamide)-1,2-ethane (bpeH<sub>2</sub>) (**2**) (270.29 g/mol, 14.06 g, 0.0520 mol, 87% yield) was prepared according to a literature procedure [118]. 1,2-Diaminoethane (60.10 g/mol,  $d = 0.899 \text{ g/ml}$ , 3.66 g, 0.060 mol, 1 equiv.) in pyridine (~12.0 ml) was added to a stirred solution of picolinic acid (123.11 g/mol, 14.76 g, 0.119 mol, 2 equiv.) in pyridine (~48.0 ml). After Triphenyl phosphite (310.29 g/mol,  $d = 1.184 \text{ g/ml}$ , 31.5 ml, 0.119 mol, 2 equiv.) was added slowly, the reaction mixture was heated for 4 h in an oil bath (100 °C). Pale yellow crystals formed overnight at room temperature. White crystals were obtained by recrystallization from Chloroform.  $^1\text{H}$  NMR (500 MHz, DMSO- $d_6$ ):  $\delta$  8.95 (s, 2H, NH<sub>2</sub>) 8.62 (d, 2H, H-1); 8.01 (d, 2H, H-4); 7.97 (td, 2H, H-3); 7.57 (td, 2H, H-5), 3.52 (m, 2H, H-5 & 6); ( $^1\text{H}$  NMR 500 MHz,  $\text{CDCl}_3$ )  $\delta$  8.52 (d, 2H, H-1), 8.37 (s, 2H, NH<sub>2</sub>), 8.16 (d, 2H, H-4), 7.80 (td, 2H, H-3), 7.38 (td, 2H, H-2), 3.73 (m, 2H, H-5 & 6).  $^{13}\text{C}$   $\{^1\text{H}\}$  NMR (125 MHz, DMSO- $d_6$ ):  $\delta$  164.16 (C=O), 149.92 (Pyridyl-*ipso*), 148.31 (C-1), 137.66 (C-3), 126.39 (C-2), 121.81 (C-4), 38.84 (C-5 & 6);  $^{13}\text{C}$   $\{^1\text{H}\}$  NMR (125 MHz,  $\text{CDCl}_3$  chloroform):  $\delta$  164.96 (C=O), 149.77 (Pyridyl-*ipso*), 148.10 (C-1), 137.25 (C-3), 126.14 (C-2), 122.21 (C-4), 39.51 (C-5 & 6).

Chloro-nitrosyl-*N,N'*-bis(2-pyridinecarboxamido)-1,3-ethane-ruthenium(II).  $[\text{Ru}(\text{NO})(\text{bpe})\text{Cl} \cdot (\text{H}_2\text{O})_2]$  (**3**) (434.84 g/mol, 0.247g,  $5.68 \times 10^{-4}$  mol, 31% yield) was prepared using an adapted procedure from Vagg and co-worker [119] **1** (0.500 g, 0.0018 mol, 1 equiv.) was added to a stirred solution of **2** (0.494 g, 0.0018 mol, 1 equiv.) in an ethanol/water solution (95%, ~60.0 ml, ~85 °C). After 12 h at reflux, a fine brown solid was filtered from the reaction mixture. Upon reduction of

solvent volume under vacuum (rotary evaporator, 30 °C) an orange solid precipitated from the filtrate. The solid was rinsed with small amounts of ethanol and dried at ~100 °C. X-ray quality crystals were obtained from a concentrated solution of [Ru(NO)(bpe)Cl·(H<sub>2</sub>O)<sub>2</sub>] in ethanol. <sup>1</sup>H NMR (500 MHz, DMSO-d<sub>6</sub>): δ 9.23 (d, 2H, H-1), 8.34 (td, 2H, H-3), 8.08 (d, H-4), 7.90 (ddd, 2H, H-2), 4.02 (m, 2H, H-5' & 6), 3.91 (m, 2H, H-5 & 6'); <sup>13</sup>C {<sup>1</sup>H} NMR (125 MHz, DMSO-d<sub>6</sub>): δ 166.56 (C=O), 157.76 (Pyridyl-*ipso*), 152.40 (C-1), 141.44 (C-3) 127.70 (C-2), 125.53 (C-4), 51.62 (C-5 & 6); IR (KBr):  $\bar{\nu}_{\text{NO}} = 1825 \text{ cm}^{-1}$ ; ESI-MS M + Na<sup>+</sup> 457.95 (M<sup>+</sup> = 434.77).

*N,N'*-bis(2-pyridine carboxamide)-1,2-propane(bppH<sub>2</sub>) (4) (284.33 g/mol, 6.75 g, 0.024 mol, 47% yield) was prepared according to a literature procedure [118]. 1,2-Diaminopropane (74.13 g/mol, *d* = 0.888 g/ml, 4.71 ml, 3.71 g, 0.050 mol, 1 equiv.) in pyridine (~20.0 ml) was added to a stirring solution of picolinic acid (123.11 g/mol, 12.3 g, 0.099 mol, 2 equiv.) in pyridine (~40 ml). After triphenyl phosphite (310.29 g/mol, *d* = 1.18 g/ml, 26.27 ml, 31.0 g, 0.099 mol, 2 equiv.) was added slowly, the reaction mixture was heated for 4 h in an oil bath ~100 °C. A brown oil was obtained after solvent evaporation (rotary evaporator, ~80 °C). The oil was dissolved in chloroform (~50 ml), washed with water (~50 ml, 3 times), saturated sodium bicarbonate solution (~50 ml, 4 times), and finally with water (~50 ml, 3 times).

The chloroform solution was dried over magnesium sulfate and concentrated under vacuum (rotary evaporator, ambient temperature). A powdery white precipitate formed as the concentrated solution was added dropwise over 1 h to diethyl ether (~70 ml, 0 °C) with stirring. Recrystallization from chloroform yielded white crystals. <sup>1</sup>H NMR (500 MHz, DMSO-d<sub>6</sub>): 8.99 (t, 2H, NH<sub>2</sub>) 8.61 (d, 2H, H-1), 8.03 (d, 2H, H-4), 7.95 (t, 2H, H-3); 7.57 (td, 2H, H-2), 3.34 (q, 4H, H-5), 1.75 (qn, 2H, H-6). <sup>13</sup>C{<sup>1</sup>H} NMR (125 MHz, DMSO-d<sub>6</sub>): δ 163.91 (C=O), 150.05 (Pyridyl-*ipso*), 148.31 (C-1), 137.68 (C-3), 126.35 (C-2), 121.79 (C-4), 36.29 (C-5), 29.42 (C-6); GC-MS *m/z* 284.

Chloronitrosyl-*N,N'*-bis(2-pyridinecarboxamido)-1,3-propane-ruthenium(II), [Ru(NO)(bpp)Cl·(H<sub>2</sub>O)<sub>2</sub>] (5) (448.86 g/mol, 0.080 g, 1.78 × 10<sup>-4</sup> mol, 10% yield), was prepared with the same procedure as described above for 3. Recrystallization from an ethanol/water solution as well as from DMSO provided X-ray quality crystals. <sup>1</sup>H NMR (500 MHz, DMSO-d<sub>6</sub>): δ 9.24 (d, 2H, H-1), 8.38 (t, 2H, H-3), 8.18 (d, H-4), 7.91(t, 2H, H-2), 3.78 (m, 2H, H-5), 3.54 (t, 2H, H-5'), 2.10 (m, 2H, H-6'), 1.77 (q, 2H, H-6); <sup>13</sup>C{<sup>1</sup>H} NMR (125 MHz, DMSO-d<sub>6</sub>): δ 168.83 (C=O), 154.23 (Pyridyl-*ipso*), 150.21 (C-1), 141.67 (C-3), 127.31 (C-2), 125.20 (C-4), 46.23 (C-5), 30.19 (C-6); IR (KBr): ( $\bar{\nu}_{\text{NO}} = 1838 \text{ cm}^{-1}$ ); ESI-MS M + Na<sup>+</sup> 471.97.

## 2.4. Crystallographic data collection

X-ray quality crystals were obtained for 3 and 5 by slow evaporation of solvent from the reaction mixture filtrate. Crystals of 5 were also obtained from DMSO after the reaction mixture filtrate was reduced in volume and taken up on DMSO. The crystal structure shown for 5 is from a crystal obtained in DMSO. Data collections were performed at room temperature on a Bruker Smart Apex CCD diffractometer using graphite-monochromated Mo K $\alpha$  ( $\lambda = 0.71073 \text{ \AA}$ ) radiation. Full crystallographic details are deposited with Cambridge Structural Database (CCD 245015 and CDC 245016). Crystal and intensity collection data can be seen in Table 1.

## 3. Results and discussion

### 3.1. Infrared data

The infrared spectrum of a pure sample of 3 in KBr showed a split nitrosyl stretch with one peak at 1852 cm<sup>-1</sup> and the other at 1825 cm<sup>-1</sup>. Split NO peaks have been observed for complexes having only one NO group. For example, splitting of the absorbance associated with the NO stretching mode has been observed for *cis*-[RuCl(en)<sub>2</sub>(NO)]Cl<sub>2</sub>, [RuBr(en)<sub>2</sub>(NO)]Br<sub>2</sub>, [RuI(en)<sub>2</sub>(NO)]I<sub>2</sub> [114], [Ru(NH<sub>3</sub>)<sub>5</sub>(NO)]Cl<sub>3</sub>·H<sub>2</sub>O [120] and *mer*-[RuX<sub>3</sub>(en)(NO)] where X = Cl, Br, and I [121] For the complex ions the splitting has been attributed to an interaction between the counterion and the NO group [21,120] Where there is no counterion, the splitting has been explained by a slight difference in the conformation of the ethylenediamine ligand induced in sample preparation [114] Unexpected peaks in infrared spectra, particularly with KBr pellets, have also been attributed to reactions with KBr and to interactions with KBr. To eliminate the possibility of some interaction with KBr as the cause of the extra NO stretch, a spectrum was obtained using a KCl pellet. With KCl the IR spectrum (Fig. 1(a)) exhibited only one NO stretch at 1825 cm<sup>-1</sup> and a shoulder of another at 1850 cm<sup>-1</sup>. It might be concluded from these data that bromide might displace chloride when the sample is prepared in KBr. Hence, only one NO peak is observed when the sample is prepared in KCl. However, the Ru-Cl bond is quite strong, especially when it is *trans* to NO. Moreover, if Br<sup>-</sup> had displaced Cl<sup>-</sup> the peak that should remain when the spectrum is obtained in KCl should be the one with the highest stretching frequency. Since the lower frequency peak remains, exchange with bromide was not the cause of the splitting. Another spectrum of the same KCl pellet of 3, obtained after several days of being exposed to air, (Fig. 1(b)) showed two NO peaks of equal intensity.

Table 1  
Crystal data and structure refinements for [Ru(NO)(bpp)Cl] **3** and [Ru(NO)(bpe)Cl] **5**

	<b>3</b>	<b>5</b>
Chemical formula	C <sub>15</sub> H <sub>18</sub> ClN <sub>5</sub> O <sub>5</sub> Ru	C <sub>14</sub> H <sub>16</sub> ClN <sub>5</sub> O <sub>5</sub> Ru
Formula weight	484.86	470.84
Temperature (K)	293(2)	295(2)
Wavelength (Å)	0.71073	0.71073
Crystal system	triclinic	triclinic
Space group	<i>P</i> $\bar{1}$	<i>P</i> $\bar{1}$
<i>a</i> (Å)	7.6860 (15)	7.3057(7)
<i>b</i> (Å)	11.180(2)	11.0170(10)
<i>c</i> (Å)	11.462(2)	11.7851(11)
$\alpha$ (°)	80.47(3)	79.900(2)
$\beta$ (°)	74.99(3)	74.622(2)
$\gamma$ (°)	72.58(3)	74.29(2)
Volume (Å <sup>3</sup> )	903.6(3)	874.93(14)
<i>Z</i>	2	2
<i>D</i> <sub>calc</sub> Mg/m <sup>3</sup>	1.767	1.787
Absorption coefficient (mm <sup>-1</sup> )	1.054	1.086
<i>F</i> (0 0 0)	480	472
Crystal size (mm <sup>3</sup> )	0.37 × 0.34 × 0.21	0.38 × 0.18 × 0.13
$\theta$ Range for data collection (°)	1.85–32.59	1.80–32.54
Index ranges	−11 ≤ <i>h</i> ≤ 11; −16 ≤ <i>k</i> ≤ 16; −17 ≤ <i>l</i> ≤ 17	−10 ≤ <i>h</i> ≤ 10; −16 ≤ <i>k</i> ≤ 16; −17 ≤ <i>l</i> ≤ 17
Reflections collected	11 590	11 486
Independent reflections ( <i>R</i> <sub>int</sub> )	6118 (0.0395)	5976 (0.0348)
Completeness	92.7% ( $\theta = 32.59^\circ$ )	94.2% ( $\theta = 32.54^\circ$ )
Data/restraints/parameters	6118/0/244	5976/0/235
Maximum and minimum transmissions	0.8091 and 0.6965	0.8717 and 0.6831
Refinement method	full-matrix least-squares on <i>F</i> <sup>2</sup>	full-matrix least-squares on <i>F</i> <sup>2</sup>
Goodness-of-fit on <i>F</i> <sup>2</sup>	1.167	1.092
Final <i>R</i> indices [ <i>I</i> > 2σ( <i>I</i> )]	<i>R</i> <sub>1</sub> = 0.0790; <i>wR</i> <sub>2</sub> = 0.2595	<i>R</i> <sub>1</sub> = 0.0615; <i>wR</i> <sub>2</sub> = 0.1487
<i>R</i> indices (all data)	<i>R</i> <sub>1</sub> = 0.0886; <i>wR</i> <sub>2</sub> = 0.2656	<i>R</i> <sub>1</sub> = 0.0870; <i>wR</i> <sub>2</sub> = 0.1606
Largest differential peak and hole (e Å <sup>3</sup> )	4.009 and −1.477	1.682 and −0.0598

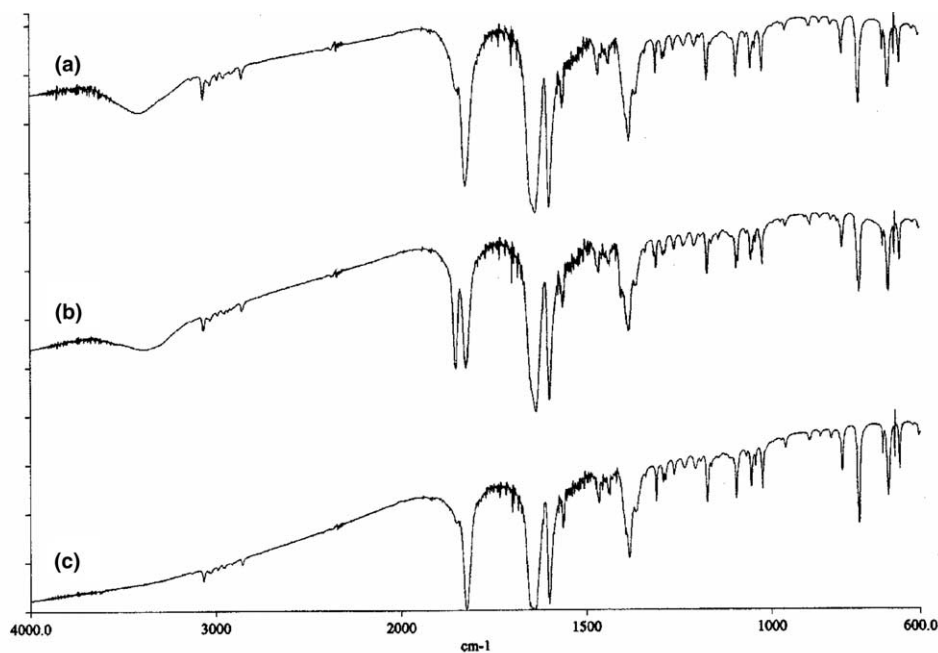


Fig. 1. IR spectrum of KCl pellet of **3**: (a) immediately after preparation; (b) after several days in air at ambient temperature; (c) after two days in 120 °C oven.

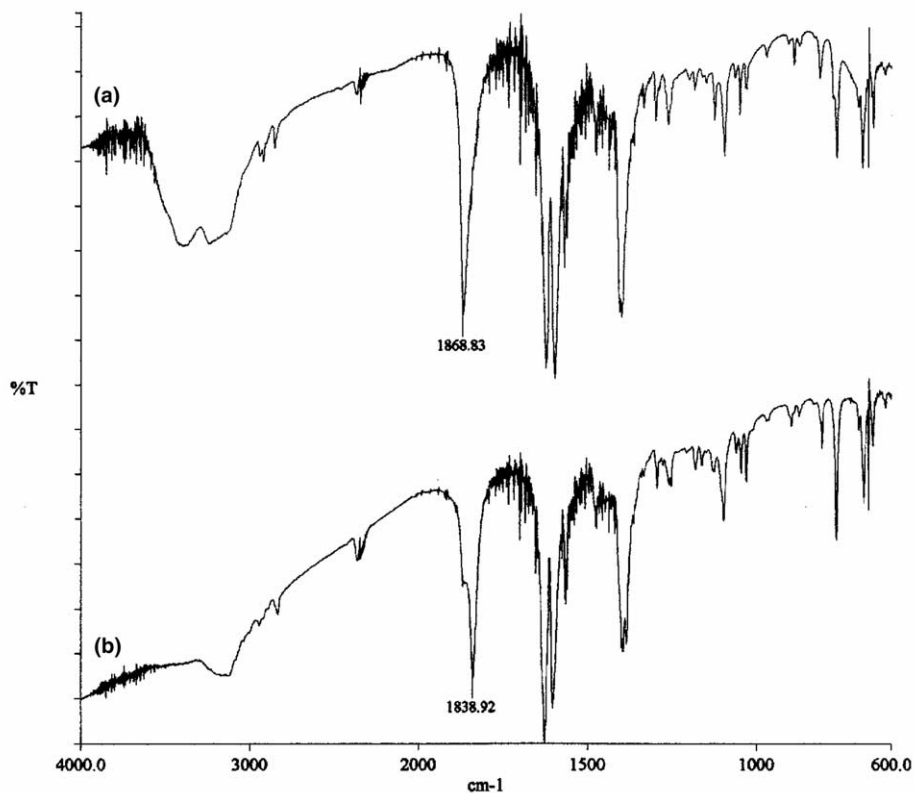


Fig. 2. (a) Fresh KBr pellet of **5**; (b) KBr pellet after 3 h at 120 °C.

The extra peak along with an increase in the intensity of the peak representing the O–H stretching mode suggested that water might be the cause of the splitting. A final IR spectrum (Fig. 1(c)), obtained after the same KCl pellet was stored for two days at 120 °C to drive off water, exhibited only one NO peak at 1825  $\text{cm}^{-1}$  and lacked the O–H peak. Therefore it was concluded that water caused the split NO peak. Only one NO peak

was observed in the infrared spectrum of **5** at 1868  $\text{cm}^{-1}$ . Given the similarity in N–O bond length, the stretching frequency for **5** seemed a little high compared to that for **3**. To test whether the one observed peak was actually two overlapping peaks, the KBr pellet of **5** was also stored at 120 °C. Fig. 2 shows that after about 3 h drying, the peak representing the NO stretching frequency had shifted to 1838  $\text{cm}^{-1}$ . In addition, as the

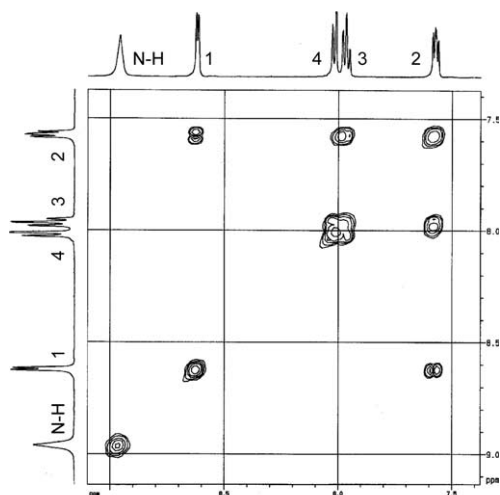


Fig. 3. Pyridyl region of HH COSY spectrum of **2**.

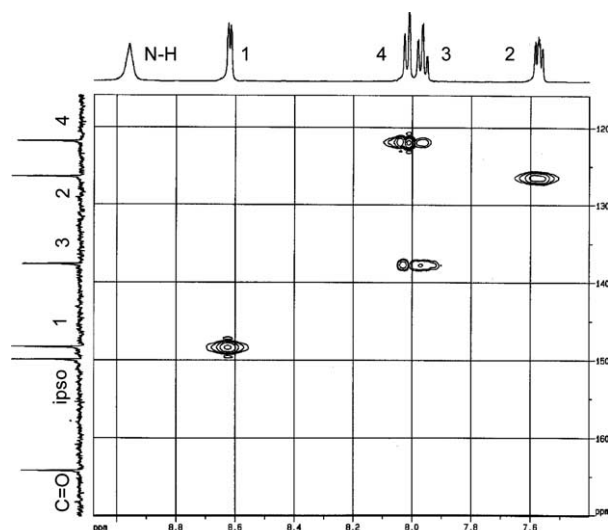
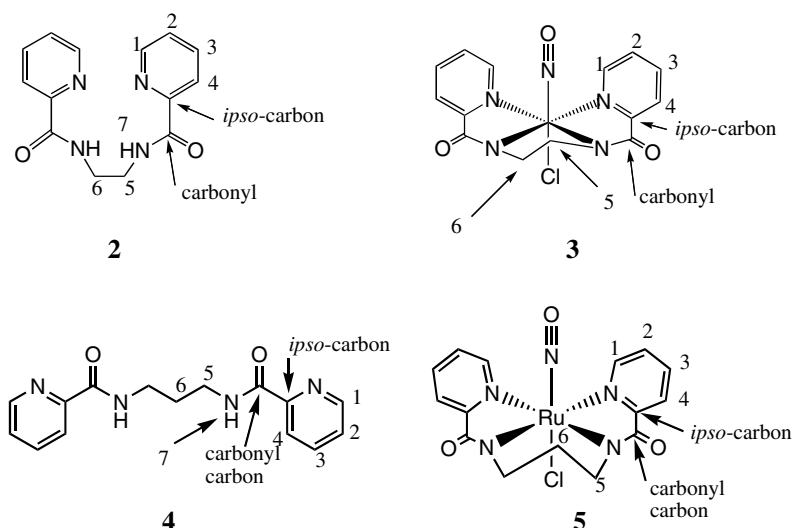


Fig. 4. Pyridyl region of HMQC spectrum of **2**.



### $^1\text{H}$ and $^{13}\text{C}$ Chemical Shifts<sup>a</sup> for **2**<sup>b</sup>, **3**<sup>c</sup>, **4**<sup>d</sup>, and **5**<sup>e</sup>

$^1\text{H}$	1	2	3	4	5	5' <sup>f</sup>	6	6' <sup>f</sup>	7		
<b>2</b>	8.62	7.57	7.97	8.01	3.52	*	3.52	*	8.95		
<b>3</b>	9.23	7.90	8.34	8.08	3.91	4.02	4.02	3.91	*		
<b>4</b>	8.61	7.57	7.95	8.03	3.34	*	1.75	*	8.99		
<b>5</b>	9.24	7.91	8.38	8.18	3.78	3.54	1.77	2.10	*		
$^{13}\text{C}$										Py- <i>ipso</i>	C=O
<b>2</b>	148.31	126.39	137.66	121.81	38.48	*	38.48	*	*	149.92	164.16
<b>3</b>	152.40	127.70	141.44	125.53	51.62	*	51.62	*	*	157.76	166.56
<b>4</b>	148.31	126.35	137.68	121.79	36.29	*	29.42	*	*	150.05	163.91
<b>5</b>	150.21	127.31	141.67	125.20	46.23	*	30.19	*	*	154.23	168.83

<sup>a</sup> 500 MHz for  $^1\text{H}$ ; 125 MHz for  $^{13}\text{C}$ ;  $\text{dms}\text{-}d_6$

<sup>b</sup> *N,N*-bis(2-pyridinecarboxamide)-1,2-ethane ( $\text{bpeH}_2$ )

<sup>c</sup>  $[\text{Ru}(\text{NO})(\text{bpe})\text{Cl}]$  ( $\text{bpe}$  = *N,N*-bis(2-pyridinecarboxamide)-1,2-ethane dianion)

<sup>d</sup> *N,N*-bis(2-pyridinecarboxamide)-1,2-propane ( $\text{bppH}_2$ )

<sup>e</sup>  $[\text{Ru}(\text{NO})(\text{bpp})\text{Cl}]$  ( $\text{bpp}$  = *N,N'*-bis(2-pyridinecarboxamide)-1,2-propane dianion)

<sup>f</sup> Prime indicates methylene proton oriented toward the Ru-NO moiety

\* Not applicable

Fig. 5.  $^1\text{H}$  and  $^{13}\text{C}$  labeling scheme and chemical shifts for **2**, **3**, **4** and **5**.

water peak decreased in size, splitting of the NO peak became apparent. A peak at about  $1384\text{ cm}^{-1}$  is characteristic of all RuNO compounds derived from  $[\text{Ru}(\text{NO})\text{Cl}_3(\text{H}_2\text{O})_2]$  is observed in the spectra for both compounds and is assigned to the Ru-NO bending mode [80].

### 3.2. NMR data

Fig. 5 shows the numbering schemes for **2**, **3**, **4** and **5** as well as the  $^1\text{H}$  and  $^{13}\text{C}$  NMR data obtained in  $\text{DMSO-}d_6$ .  $^1\text{H}$  and  $^{13}\text{C}$  assignments are based on the HH COSY and HMQC spectra. The HH COSY and HMQC spectra for the pyridyl resonances of **2** are

shown in Figs. 3 and 4, respectively. Fig. 3 depicts the correlations between H-2, H-3 and H-1 and between H-3 and H-4. A correlation (not shown) also exists between the ethylene protons at 3.52 ppm and the amide protons at 8.95 ppm.

The HMQC spectrum in Fig. 4 shows the correlation of each proton resonance with its respective carbon resonance. Quaternary carbon signals at 149.77 and 164.96 ppm in the HMQC spectrum are assigned to the pyridyl-*ipso* carbon and the carbonyl carbon, respectively, based upon the HMBC spectrum.<sup>1</sup> The most downfield  $^{13}\text{C}$  signal that exhibits a proton correlation appears at

<sup>1</sup> HMBC Spectrum can be seen in the supplementary information.

148.10 ppm and corresponds to H-1. H-1 is also the most downfield doublet by virtue of its proximity to electron withdrawing the pyridyl nitrogen. The next most downfield doublet, H-4, correlates with the second most upfield  $^{13}\text{C}$  resonance. This may be rationalized by considering the magnetic anisotropy induced by the ring current as well as the different resonance forms of the pyridine ring [122,123]. Except for the extra carbon and proton signals associated with the extra methylene carbon in **4**, the NMR data for **4** is almost exactly the same as that for **2**.

Fig. 5 compares the  $^1\text{H}$  and  $^{13}\text{C}$  data for **2**, **3**, **4** and **5**. The lack of an N–H signal in the  $^1\text{H}$  NMR spectra for **3** and **5** indicates that each ligand coordinates in its deprotonated form. Due to the electron withdrawing nature of the Ru–NO center [80], all proton and carbon resonances shift downfield upon coordination to ruthenium. The ethylene carbon atoms are undifferentiated in the  $^{13}\text{C}$  spectrum of **3**, however the protons associated with them, H-5 and H-6, are differentiated by their proximity to the nitrosyl group [69,121]. Fig. 6 illustrates how the ethylene protons' signal splits into two downfield shifted multiplets upon formation of **3**. The most downfield multiplet at 4.02 ppm is assigned to H-5', the axial proton on carbon 5 and to H-6, the equatorial proton on C-6. The signal at 3.90 ppm represents H-5 and H-6', which are on the chloride face of the compound and farthest from the NO group. It may be helpful to refer to the crystal structure of **3** in Fig. 7; but be aware of the different numbering scheme.

In **4** the protons on C-5, which are bonded to the amido nitrogens, are identical to each other; however, they are in different environments than those on the central methylene carbon, C-6. Thus the spectrum exhibits a triplet at 3.34 ppm for protons labeled H-5 and a multiplet at 1.75 ppm for protons labeled H-6. Coordination of **4** causes both methylene signals to shift downfield and split into two groups of two signals. One of the signals, a doublet of doublets, at 3.78 ppm, has been assigned to

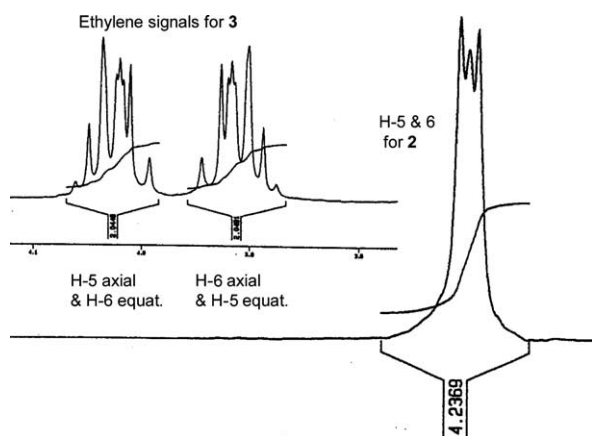


Fig. 6. Ethylene protons' signal for **2** splits into two multiplets upon formation of **3**.

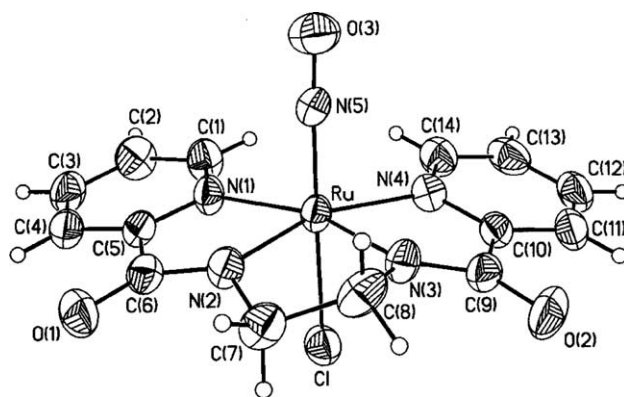


Fig. 7. Molecular structure of **3** [Ru(NO)(bpe)Cl] (bpe = *N,N'*-bis(2-pyridinecarboxamide)-1,2-ethane dianion).

the protons that are directed toward the nitrosyl group; the other signal, an apparent triplet at 3.54 ppm has been assigned to those oriented toward the chloride. The central methylene resonance is also split into two multiplets. Again, the most downfield shifted signal at 2.10 ppm has been assigned to the proton which is directed toward the nitrosyl group while the negligibly shifted resonance at 1.77 ppm is assigned to the proton directed away from the NO group.

As previously mentioned, all  $^1\text{H}$  and  $^{13}\text{C}$  signals for shift downfield upon coordination. However there are some interesting differences in the magnitude of the shift for **3** and **5**. For **3** both carbons which are bonded to the amido nitrogen atoms (C-5) resonate 13.14 ppm more downfield than those of the free ligand. This compares to a downfield shift of 9.94 ppm for the analogous carbon atoms in **5**. Also, C-1 and the pyridyl *ipso* signals are more affected upon coordination in **3** than they are in **5**. For **3** for C-1 shifts 4.09 ppm, while that for **5** C-1 shifts only 1.9 ppm. A difference of similar magnitude is seen for the pyridyl *ipso* carbon which is downfield shifted 7.84 ppm in **3** and only 4.18 ppm for **5**. The carbonyl signal, on the other hand, is less responsive to coordination in **3** than it is in **5**. In **3** the carbonyl carbon

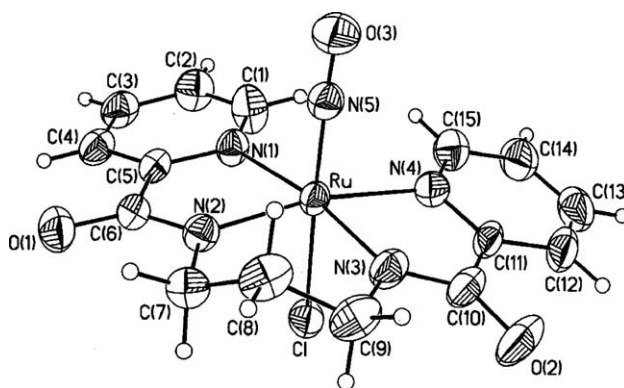


Fig. 8. Molecular structure of **5** [Ru(NO)(bpp)Cl] (bpp = *N,N'*-bis(2-pyridinecarboxamide)-1,2-propane dianion).

Table 2  
Selected bond distances (Å) and bond angles (°) for 3

O(3)–N(5)	1.140(5)	O(2)–C(9)	1.238(5)
Ru–N(5)	1.742(4)	O(1)–C(6)	1.231(5)
Ru–Cl	2.3833(12)	N(2)–C(7)	1.471(6)
Ru–N(1)	2.118(3)	C(7)–C(8)	1.532(8)
Ru–N(4)	2.127(4)	N(3)–C(8)	1.456(6)
Ru–N(3)	1.980(3)	N(3)–C(9)	1.315(6)
Ru–N(2)	1.983(4)	N(2)–C(6)	1.329(6)
O(3)–N(5)–Ru	177.0(4)	N(3)–Ru–N(4)	79.51(15)
N(5)–Ru–Cl	174.18(13)	N(3)–Ru–N(1)	162.58(15)
N(5)–Ru–N(1)	92.53(16)	N(2)–Ru–N(4)	161.11(15)
N(5)–Ru–N(4)	92.81(16)	C(8)–N(3)–Ru	112.5(3)
N(5)–Ru–N(3)	96.39(16)	N(3)–C(8)–C(7)	110.4(4)
N(5)–Ru–N(2)	98.48(17)	C(7)–N(2)–Ru	113.4(3)
N(3)–Ru–N(2)	84.20(15)	N(2)–C(7)–C(8)	109.3(4)
N(1)–Ru–N(4)	115.04(14)	N(3)–C(9)–C(10)	112.2(4)
N(2)–Ru–N(1)	79.70(14)	N(2)–C(6)–C(5)	112.7(4)

Table 3  
Selected bond distances (Å) and angles (°) for 5

O(3)–N(5)	1.143(8)	O(1)–C(6)	1.246(8)
Ru–N(5)	1.732(6)	O(2)–C(10)	1.252(9)
Ru–Cl	2.3683(19)	N(2)–C(6)	1.321(9)
Ru–N(1)	2.129(5)	N(3)–C(10)	1.298(10)
Ru–N(4)	2.147(7)	N(2)–C(7)	1.460(9)
Ru–N(3)	2.039(6)	C(7)–C(8)	1.517(11)
Ru–N(2)	2.034(6)	C(8)–C(9)	1.522(13)
		N(3)–C(9)	1.468(10)
O(3)–N(5)–Ru	177.5(7)	N(3)–Ru–N(4)	77.9(3)
N(5)–Ru–Cl	176.4(2)	N(3)–Ru–N(1)	171.1(2)
N(5)–Ru–N(1)	93.2(3)	N(2)–Ru–N(4)	169.0(2)
N(5)–Ru–N(4)	93.3(3)	N(2)–C(7)–C(8)	112.6(6)
N(5)–Ru–N(3)	93.7(3)	C(7)–C(8)–C(9)	115.8(7)
N(5)–Ru–N(2)	95.9(3)	C(9)–N(3)–Ru	123.4(5)
N(2)–Ru–N(3)	95.4(3)	C(7)–N(2)–Ru	123.5(5)
N(1)–Ru–N(4)	107.3(2)	N(3)–C(10)–C(11)	114.1(6)
N(2)–Ru–N(1)	78.3(2)	N(2)–C(6)–C(5)	113.5(6)

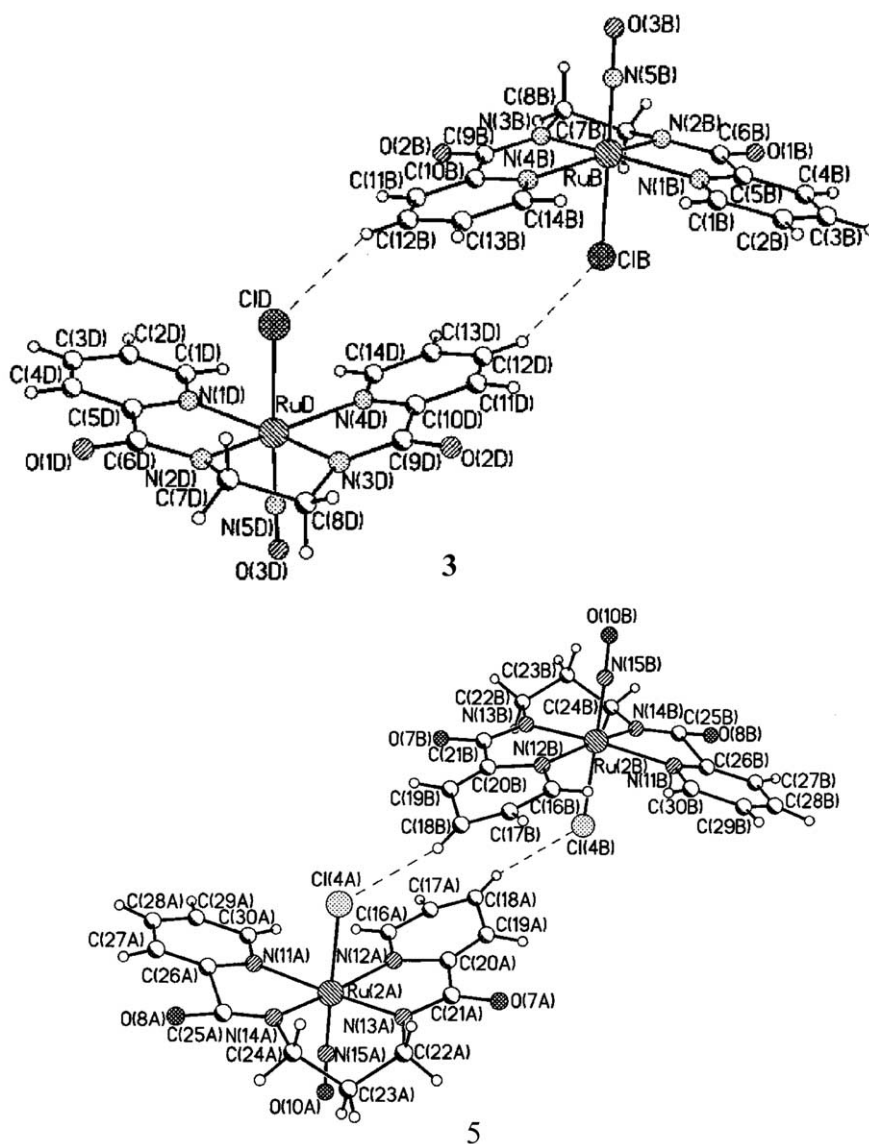


Fig. 9. Close contacts in the crystal lattices of [Ru(NO)(bpe)Cl] 3 and [Ru(NO)(bpp)Cl] 5.

$^{13}\text{C}$  signal shifts downfield 2.40 ppm while in **5** it shifts 4.92 ppm.

### 3.3. Crystal structure data

Figs. 7 and 8 display the molecular structures of **3** and **5**, respectively. Tables 2 and 3 show selected bond lengths and angles for **3** and **5**, respectively. That **3** and **5** are crystallographic isomorphs facilitates a direct comparison of the two structures. Both the pyridyl and deprotonated amido nitrogen atoms of the tetradentate  $\text{bpe}^{2-}$  and  $\text{bpp}^{2-}$  ligands coordinate to the ruthenium center in the equatorial plane to form a slightly distorted octahedral compound with axial chloride and nitrosyl substituents. The Ru–N amido and the Ru–N pyridyl bonds are all shorter in **3** than in **5**. The C–O bond lengths are shorter in **3** than in **5** as well. The Ru–N–O angle in each compound is essentially linear at  $177.0(4)$  for **3** and  $177.5(6)$  for **5**. It follows that the N–O bond length for **3** ( $1.140(5)$  Å) is very similar to that for **5** ( $1.143(8)$  Å). That the Ru–NO ( $1.732(6)$  Å) and Ru–Cl ( $2.368(3)$  Å) bond lengths for **5** are slightly shorter than those in **3** Ru–NO ( $1.742(4)$  Å) and Ru–Cl ( $2.3833(12)$  Å) may indicate that the NO group exerts a slightly stronger *trans* strengthening effect in **3** than in **5**. The longer Ru–Cl and Ru–N(5) bonds in **3** may also be due to the smaller bite angles of the  $\text{bpe}^{2-}$  ligand as discussed below.

The ruthenium center is displaced toward the nitrosyl group from the plane defined by the nitrogen atoms ( $0.145$  Å in **5** and  $0.167$  Å in **3**) due to the different bite angles of the ligands. More displacement is required to alleviate the steric interaction with the rings in **3** because the five member chelate ring has a smaller bite angle ( $84.20(15)^\circ$ ) [19]. The smaller N(2)–Ru–N(3) angle in **3** also allows a larger N(1)–Ru–N(4) angle of  $115.04(14)$  Å. The six member chelate ring in **5**, which has a bite angle of  $95.4(3)^\circ$ , forces a smaller N(1)–Ru–N(4) angle of  $107.3(2)^\circ$ . The smaller N(1)–Ru–N(4) in **5** causes the pyridyl groups to tip out of the plane slightly more in **5** than in **3** to minimize steric interaction between H-1 and H-14. Tilting of chelated pyridyl groups has been observed by others [89]. Both pyridyl rings involving N(1) on **3** and **5** exhibit less of a tilt than do those involving N(4).

The carbon–carbon bonds in the 5 member ring formed by the diamide in **3** exhibit typical bond lengths and angles. The N(5)–Ru–N(2) angle is  $98.48(17)^\circ$  while the N(5)–Ru–N(3) angle is a little less at  $96.35(16)^\circ$ . The six member ring formed upon chelation of the  $\text{bpp}^{2-}$  ligand exhibits angles that are little larger than those of a six member ring. The largest deviation from the typical value of  $112^\circ$  is the C(8)–C(9)–N(3) angle which is  $115.87^\circ$ . In **5** the N(5)–Ru–N(2) and N(5)–Ru–N(3) angles, at  $95.9(3)^\circ$  and  $93.7(3)^\circ$ , respectively, deviate less from  $90^\circ$  than do those in **3**.

Finally, as Fig. 9 shows, there are short close contacts between the chloride ion and the hydrogen atom on the pyridyl ring that is para to the nitrogen of the heterocycle. This interaction is significant enough to pull the hydrogen atoms attached to C-10 in **3** and C-12 in **5** slightly out of the plane of the rest of the pyridyl hydrogen atoms.

### 4. Conclusions

The  $\{\text{RuNO}\}^6$  compounds,  $[\text{Ru}(\text{NO})(\text{bpe})\text{Cl} \cdot 2\text{H}_2\text{O}]$  and  $[\text{Ru}(\text{NO})(\text{bpp})\text{Cl} \cdot 2\text{H}_2\text{O}]$ , are distorted octahedral compounds with the chloride ligand *trans* to a linearly bound NO group. The  $^1\text{H}$  and  $^{13}\text{C}$  spectra suggest that the compounds maintain the same coordination geometry in solution as they do in the solid state. The crystal structure reveals that all of the ruthenium nitrogen bonds in the equatorial plane are shorter for **3** than for **5**. Accordingly  $^{13}\text{C}$  and  $^1\text{H}$  NMR analyses show that nitrogen bound carbons and their respective protons are more downfield shifted in **3** than in **5** upon coordination. An exception is the  $^{13}\text{C}$  signal of the carbonyl carbon which is less downfield shifted in upon coordination of **3** than it is upon coordination of **5**.

The nitrosyl stretching frequencies of  $1825\text{ cm}^{-1}$  for **3** and  $1838\text{ cm}^{-1}$  for **5** are in good agreement with literature values for similar compounds [12,44,89,114]. That the NO stretching frequencies of **3** and **5** are less than that for the  $[\text{Ru}(\text{NO})(\text{bpb})\text{Cl}]$  compound ( $1867\text{ cm}^{-1}$ ) indicates that more electron density is pushed on to the NO group by the  $\text{bpe}^{2-}$  and the  $\text{bpp}^{2-}$  ligand than by the  $\text{bpb}^{2-}$  ligand.

The infrared spectrum of **3** exhibited a distinctly split NO peak. Split NO peaks have been observed and attributed to interactions with counter ions, slight variations in NO and ligand conformation, solvent when the sample is prepared in solution, and with reactions with KBr in KBr pellets [10,124,125]. The split NO peak exhibited by **3** is attributed to a hydrogen bonding interaction with water in the KBr pellet. Drying the KBr pellet of **5** revealed that there was a split NO peak for **5** as well. Drying of a KBr pellet of  $[\text{Ru}(\text{NO})(\text{bpb})\text{Cl}]$  removed water but the NO peak remained unchanged. This may indicate that the nitrosyl oxygen atoms in **3** and in **5** exhibit a higher basicity, therefore an increased propensity to hydrogen bond [126], compared to that in  $[\text{Ru}(\text{NO})(\text{bpb})\text{Cl}]$ . Photolysis and electrochemical studies of **3** and **5** are in progress.

### Acknowledgements

Support from the Petroleum Research Fund is gratefully acknowledged. C.F.F. also wishes to thank the University of Pittsburgh's Chemistry Department for

the opportunity to continue Dr. Shepherd's research. C.F.F. is especially grateful to Professors Bodie E. Douglas, David H. Waldeck, Stéphane Petoud, and Stephen G. Weber whose efforts have made this research possible.

## Appendix A. Supplementary data

Supplementary data associated with this article can be found, in the online version at [doi:10.1016/j.ica.2004.09.060](https://doi.org/10.1016/j.ica.2004.09.060).

## References

- [1] J.H. Enemark, R.D. Feltham, *Coord. Chem. Rev.* 13 (1974) 339.
- [2] R.D. Feltham, J.H. Enemark, in: G. Geoffroy (Ed.), *Topics in Inorganic and Organometallic Stereochemistry*, vol. 12, Wiley, New York, 1981, pp. 155–215.
- [3] B.L. Westcott, J.H. Enemark, in: E.I. Solomon, A.B.P. Lever (Eds.), *Inorganic Electronic Spectroscopy*, vol. II, Wiley, New York, 1999, pp. 403–450.
- [4] B.L. Haymore, J.A. Ibers, *Inorg. Chem.* 14 (1975) 3060.
- [5] R. Hoffman, M.M.L. Chen, E. Mihai, A.R. Rossi, D.M.P. Mingos, *Inorg. Chem.* 13 (1974) 2666.
- [6] D.M.P. Mingos, *Inorg. Chem.* 12 (1973) 1209.
- [7] D.M.P. Mingos, L.K. Bell, J. Mason, D.G. Tew, *Inorg. Chem.* 22 (1983) 3497.
- [8] C.G. Pierpont, D.G. Van Derveer, W. Durland, R. Eisneberg, *J. Am. Chem. Soc.* 92 (1970) 4760.
- [9] C.G. Pierpont, A. Pucci, R. Eisneberg, *J. Am. Chem. Soc.* (1971) 3050–3051.
- [10] G.B. Richter-Addo, P. Legzdins, *Metal Nitrosyls*, Oxford University Press, New York, 1992.
- [11] A.F. Cotton, G. Wilkinson, C.A. Murillo, M. Bochmann, *Advanced Inorganic Chemistry*, sixth ed., Wiley, New York, 1999.
- [12] A.F. Schreiner, S.W. Lin, P.J. Hauser, E.A. Hopcus, D.J. Hamm, J.D. Gunter, *Inorg. Chem.* 11 (1972) 880.
- [13] B.J. Coe, S.J. Glenwright, *Coord. Chem. Rev.* 203 (2000) 5.
- [14] T. Hirano, T. Oi, H. Nagao, K. Morokuma, *Inorg. Chem.* 42 (2003) 6575.
- [15] T. Kimura, T. Sakurai, T. Shima, M. Togano, M. Mukaida, T. Nomura, *Inorg. Chim. Acta* 69 (1983) 135.
- [16] E. Miki, K. Harada, Y. Kamata, M. Umehara, K. Mizumachi, M. Tanaka, T. Nagai, T. Ishimori, M. Nakahara, *Polyhedron* 10 (1991) 583.
- [17] H. Nishimura, H. Matsuzawa, T. Togano, M. Mukaida, H. Kakihana, F. Bottomley, *J. Chem. Soc., Dalton Trans.* (1990) 137–141.
- [18] N.M. Sinityn, O.E. Zvyagintsev, *Dokl. Akad. Nauk SSSR* 145 (1962) 109.
- [19] H. Tomizawa, E. Miki, K. Mizumachi, T. Ishimori, *Bull. Chem. Soc. Jpn.* 67 (1994) 1816.
- [20] J.T. Veal, D.J. Hodgson, *Acta. Crystallogr. B* 28 (1972) 3525–3529.
- [21] E.Y. Bobkova, N.B. Borkovskii, A.A. Svetlov, G.G. Novitskii, *Russ. J. Inorg. Chem.* 39 (1994) 796.
- [22] L. Andrews, A. Citra, *Chem. Rev.* 102 (2002) 885.
- [23] A.A. Levin, *J. Mol. Struct.* 272 (1992) 133.
- [24] O.V. Sizova, V.I. Baranovski, N.V. Ivanova, V.V. Sizov, *Mol. Phys.* 101 (2003) 715.
- [25] D. Chatterjee, A. Mitra, R.E. Shepherd, *Inorg. Chim. Acta* 357 (2004) 980.
- [26] J.P. Collman, *Acc. Chem. Res.* 1 (1968) 136.
- [27] J.P. Collman, N.W. Hoffman, D.E. Morris, *J. Am. Chem. Soc.* 91 (1969) 5659.
- [28] A. Katho, Z. Opre, L. Gabor, J. Ferenc, G. Lawrenczy, T. Goo, *J. Mol. Cat. A: Chem.* 204–205 (2003) 143–148.
- [29] D.M.P. Mingos, D.J. Sherman, in: A.G. Sykes (Ed.), *Advances in Inorganic Chemistry*, vol. 34, Harcourt, Brace and Jovanovich, London, 1989, pp. 293–377.
- [30] A. Miyata, M. Murakami, R. Irie, T. Katsuki, *Tet. Lett.* 42 (2001) 7067.
- [31] W. Odenkirk, A.L. Rheingold, B. Bosnich, *J. Am. Chem. Soc.* 114 (1992) 6392.
- [32] S.T. Wilson, J.A. Osborn, *J. Am. Chem. Soc.* 93 (1971) 3068.
- [33] R.F. Furchgott, in: C. Owman, J.E. Hardebo (Eds.), *Neural Regulation of Brain Circulation*, Elsevier, New York, 1986, p. 3.
- [34] R.F. Furchgott, *Ann. Rev. Pharmacol. Toxicol.* 35 (1995) 1.
- [35] R.F. Furchgott, *Angew. Chem. Int. Ed.* 38 (1999) 1870.
- [36] L.J. Ignarro, *Nitric Oxide Biology and Pathobiology*, Academic Press, New York, 2000.
- [37] G. Stochel, A. Wanat, E. Kulis, Z. Stasicka, *Coord. Chem. Rev.* 171 (1998) 203.
- [38] P.C. Ford, M. Hoshino, L. Laverman, *Coord. Chem. Rev.* 187 (1999) 75.
- [39] D.R. Lang, J.A. Davis, L.G.F. Lopes, A.A. Ferro, L.C.G. Vasconcellos, D.W. Franco, E. Tfouni, A. Wieraszko, M.J. Clarke, *Inorg. Chem.* 39 (2000) 2294.
- [40] M.G. Gomes, C.U. Davanzo, S.C. Silva, L.G.F. Lopes, P.S. Santos, D.W. Franco, *J. Chem. Soc., Dalton Trans.* 4 (1998) 601.
- [41] C.F. Works, C.J. Jocher, G.D. Bart, B. Xianhui, P.C. Ford, *Inorg. Chem.* 41 (2002) 3728.
- [42] C.F. Works, P.C. Ford, *J. Am. Chem. Soc.* 122 (2000) 7592.
- [43] R. Ackroyd, C. Kelty, N. Brown, M. Reed, *Photochem. Photobiol.* 74 (2001) 656.
- [44] J. Bordini, D.L. Hughes, J.D. Da Motta Neto, C.J. da Cunha, *Inorg. Chem.* (2002) 5410.
- [45] J. Bourassa, W. DeGraff, S. Kudo, D.A. Wink, J.B. Mitchell, P.C. Ford, *J. Am. Chem. Soc.* 119 (1997) 2853.
- [46] P. Coppens, I. Novozhilova, A. Kovalevsky, *Chem. Rev.* 120 (2002) 861.
- [47] P.C. Ford, J. Bourassa, K. Miranda, B. Lee, I. Lorkovic, S. Boggs, S. Kudo, L. Laverman, *Coord. Chem. Rev.* 171 (1998) 185.
- [48] R.R. Hill, J.D. Coyle, D. Birch, E. Dawe, G.E. Jeffs, D. Randall, I. Stec, T.M. Stevenson, *J. Am. Chem. Soc.* 113 (1991) 1805.
- [49] M. Hoshino, S. Arai, Y. Yamaji, *J. Phys. Chem.* 90 (1986) 2109.
- [50] M. Hoshino, K. Ozawa, H. Seki, P.C. Ford, *J. Am. Chem. Soc.* 115 (1993) 9568.
- [51] J.B. Mitchell, D.A. Wink, W. Degraff, J. Gamson, L.K. Keefer, M.C. Krishna, *Canc. Res.* 53 (1993) 5845.
- [52] E.G. Moore, Q.H. Gibson, *J. Biol. Chem.* 251 (1976) 2788.
- [53] E.A. Morlino, M.A.J. Rodgers, *J. Am. Chem. Soc.* 118 (1996) 11798.
- [54] J.I. Zink, *Photochem. Photobiol.* 65 (1997) 65.
- [55] B. Mayer, *Handbook of Experimental Pharmacology*, Springer-Verlag, Berlin, 2000.
- [56] N. Toda, S. Moncada, R.F. Furchgott, E.A. Higgs, *Nitric Oxide and the Peripheral Nervous System*, Portland Press, London, 2000.
- [57] A. Kitabatake, I. Sakuma, *Recent Advances in Nitric Oxide Research*, Springer-Verlag, Tokyo, 1999.
- [58] J.D. Laskin, D.L. Laskin, *Cellular and Molecular Biology of Nitric Oxide*, Marcel Dekker, New York, 1999.
- [59] S. Moncada, G. Nistico, G. Bagetta, E.A. Higgs, *Nitric Oxide and the Cell Proliferation, Differentiation and Death*, Princeton University Press, Princeton, NJ, 1998.

- [60] A. Titheradge, Nitric Oxide Protocols, vol. 100, Humana Press, Totowa, NJ, 1998.
- [61] J. Lincoln, C.H.V. Hoyle, G. Burnstock, Nitric Oxide in Health and Disease, vol. 1, Cambridge University Press, New York, 1997.
- [62] Y.A. Henry, A. Guissani, B. Ducastel, Nitric Oxide Research From Chemistry to Biology EPR Spectroscopy of Nitrosylated Compounds, Landes Company and Chapman & Hall, Austin, 1997.
- [63] J. Lancaster, Nitric Oxide Principles and Actions, Academic Press, San Diego, 1996.
- [64] L. Packer, in: John N. Abelson, M.I. Simon (Eds.), Methods in Enzymology, vol. 269, Academic Press, New York, 1996.
- [65] C. Nathan, D.V. Madison, E.M. Schuman, R. Busse, I. Fleming, V.B. Schini, J.S. Stamler, H. Maeda, T. Akaike, M. Yoshida, K. Sato, Y. Noguchi, B. Dietzshold, J.P. Crow, J.S. Beckman, H.H.H.W. Schmidt, H. Hofmann, P. Ogilvie, in: H. Koprowski, H. Maeda (Eds.), Current Topics in Microbiology and Immunology, vol. 196, Springer-Verlag, Heidelberg, 1995.
- [66] E. Tfouni, M. Krieger, B.R. McGarvey, D.W. Franco, Coord. Chem. Rev. 236 (2003) 57.
- [67] G.B. Richter-Addo, P. Legzdins, J. Burstyn, Chem. Rev. 102 (2002) 857.
- [68] S.P. Fricker, Plat. Met. Rev. 39 (1995) 150.
- [69] F. Bottomley, Coord. Chem. Rev. 26 (1978) 7.
- [70] P.L. Feldman, O.W. Griffith, D.J. Stuehr, Chem. Eng. News 71 (1993) 26.
- [71] F. Bottomley, in: P.S. Braterman (Ed.), Reactions of Coordinated Ligands, vol. 2, Plenum Press, New York, 1986, p. 115.
- [72] Y. Chen, R.E. Shepherd, Inorg. Chim. Acta 343 (2003) 281.
- [73] Y. Chen, F.T. Lin, R.E. Shepherd, Inorg. Chem. 38 (1999) 973.
- [74] R.E. Shepherd, J.M. Slocik, T.W. Stringfield, K.V. Somayajula, A.A. Amoscato, Inorg. Chim. Acta 357 (2004) 965.
- [75] T.W. Stringfield, K.V. Somayajula, D.C. Muddiman, J.W. Flora, R.E. Shepherd, Inorg. Chim. Acta 343 (2003) 317.
- [76] J.M. Slocik, R.A. Kortess, R.E. Shepherd, Met. Based Drugs 7 (2001) 67.
- [77] J.M. Slocik, K.V. Somayajula, R.E. Shepherd, Inorg. Chim. Acta 320 (2001) 148.
- [78] J.M. Slocik, M.S. Ward, K.V. Somayajula, R.E. Shepherd, Trans. Met. Chem. 26 (2001) 351.
- [79] J.M. Slocik, R.E. Shepherd, Inorg. Chim. Acta 311 (2000) 80.
- [80] J.M. Slocik, M.S. Ward, R.E. Shepherd, Inorg. Chim. Acta 317 (2001) 290.
- [81] T.W. Stringfield, K.V. Somayajula, D.C. Muddiman, J.W. Flora, R.E. Shepherd, Inorg. Chim. Acta 343 (2003) 317.
- [82] M.S. Ward, F.T. Lin, R.E. Shepherd, Inorg. Chim. Acta 343 (2003) 231.
- [83] C.F. Fortney, R.E. Shepherd, Inorg. Chem. Commun. 7 (2004) 1065.
- [84] D.W. Pipes, T.J. Meyer, Inorg. Chem. 23 (1984) 2466.
- [85] P.C. Ford, Coord. Chem. Rev. 5 (1970) 75.
- [86] W.C. Silva, E.E. Castellano, D.W. Franco, Polyhedron 23 (2004) 1063.
- [87] C. Bremard, G. Nowogrocki, S. Sœur, Inorg. Chem. 18 (1979) 1549.
- [88] J.E. Huheey, Inorganic Chemistry Principles of Structure and Reactivity, second ed., Harper & Row, New York, 1978.
- [89] A.K. Patra, M.J. Rose, K.A. Murphy, M.M. Olmstead, P.K. Mascharak, Inorg. Chem. 43 (2004) 4487.
- [90] R. Shepherd, Personal Communication.
- [91] R.E. Shepherd, in: 35th Central Regional Meeting of the American Chemical Society, American Chemical Society, Pittsburgh, PA, 2003.
- [92] P. Comba, W. Goll, B. Nuber, K. Varnagy, Eur. J. Inorg. Chem. (1998) 2041.
- [93] T. Gajda, B. Henry, J. Delpuech, A. Aubrey, J. Inorg. Biochem. 35 (1996) 586.
- [94] R.W. Hay, M.M. Hassan, J. You-Quan, Inorg. Biochem. 52 (1993) 17.
- [95] L. Pickart, J.H. Freedman, W.J. Loker, C.J. Peisach, C.M. Perkins, R.E. Stenkamp, B. Weinstein, Nature 288 (1980) 715.
- [96] S. Kasselflouri, J.P. Laussac, N. Hadjiliadis, Inorg. Chim. Acta 166 (1989) 239.
- [97] N. Camerman, A. Camerman, B. Sarkar, Can. J. Chem. 54 (1976) 1309.
- [98] M.J. Clarke, Z. Fuchun, D.R. Frasca, Chem. Rev. 99 (1999) 2511.
- [99] W. Peti, T. Pieper, M. Sommer, B.K. Keppler, G. Geister, Eur. J. Inorg. Chem. 9 (1999) 1555.
- [100] R.A. Vilaplana, F. Gonzalez-Vilchez, E. Gutierrez-Puebla, C. Ruiz-Valero, Inorg. Chim. Acta 224 (1994) 15.
- [101] G. Sava, S. Pacor, F. Bregant, A. Ceschia, Anticancer Res. 11 (1991) 1103.
- [102] B.K. Keppler, W. Rupp, U.M. Juhl, H. Endres, R. Niebel, W. Balzer, Inorg. Chem. 26 (1987) 4366.
- [103] M.J. Clarke, in: S.J. Lippard (Ed.), Platinum, Gold and Other Chemotherapeutic Agents, ACS, Washington, DC, 1983, p. 335.
- [104] R.L. Chapman, F. Stephens, R.S. Vagg, Inorg. Chim. Acta 52 (1981) 161.
- [105] H.C. Freeman, Adv. Protein Chem. 22 (1967) 257.
- [106] L. Fabbri, T.A. Kaden, A. Perotti, B. Seghi, L. Siegfried, Inorg. Chem. 25 (1994) 321.
- [107] M.J. Upadhyay, P.K. Bhattacharya, P.A. Ganeshpure, S. Satish, J. Mol. Cat. A: Chem. 88 (1994) 287.
- [108] T.J. Collins, R.D. Powell, C. Slebodnick, E.S. Uffelman, J. Am. Chem. Soc. 112 (1990) 899.
- [109] D.W. Margerum, Pure Appl. Chem. 55 (1983) 23.
- [110] R.E. Shepherd, in: Metal-Medicine Course, University of Ioannina, Ioannina, Greece, 2003.
- [111] F.G. Marcondes, A.A. Ferro, A. Souza-Torsoni, M. Sumitani, M.J. Clarke, D.W. Franco, E. Tfouni, M. Krieger, Nitric Oxide 4 (2000) 181.
- [112] D.W. Franco, E. Tfouni, M. Krieger, J.C. Toledo, B. Barros, Nitric Oxide 4 (2000) 254.
- [113] A.A. Batista, C. Pereira, S.L. Queiroz, L.A.A. de Oliveira, R.H. de A. Santos, T. do P. Gambardella, Polyhedron 16 (1997) 927.
- [114] H. Tomizawa, E. Miki, K. Mizumachi, I. Tatsujiro, Bull. Chem. Soc. Jpn. 67 (1994) 1809.
- [115] S.K. Dutta, U. Beckmann, E. Bill, T. Weyhermuller, K. Wieghardt, Inorg. Chem. 39 (2000) 3355.
- [116] R.L. Chapman, F. Stephens, R.S. Vagg, Inorg. Chim. Acta 43 (1980) 29.
- [117] J.M. Fletcher, I.L. Jenkins, F.M. Lever, F.S. Martin, A.R. Powell, R. Todd, J. Inorg. Nucl. Chem. 1 (1955) 378.
- [118] D.J. Barnes, R.L. Chapman, R.S. Vagg, E.C. Walton, J. Chem. Eng. Data 23 (1978) 349.
- [119] R.L. Chapman, R.S. Vagg, Inorg. Chim. Acta 33 (1979) 227.
- [120] F. Bottomley, J. Chem. Soc., Dalton Trans. (1974) 1600.
- [121] H. Tomizawa, K. Harada, E. Miki, K. Mizumachi, T. Ishimori, Bull. Chem. Soc. Jpn. 66 (1993) 1658.
- [122] R.R. Gupta, M. Kumar, V. Gupta, Heterocyclic Chemistry, vol. I, Springer-Verlag, Heidelberg, 1998.
- [123] M. Jones, Organic Chemistry, W.W. Norton & Company, New York, 2000.
- [124] G.S. Girolami, T.B. Rauchfuss, R.J. Angelici, Synthesis and Technique in Inorganic Chemistry, third ed., University Science Books, Sausalito, 1999.
- [125] P.B. Coleman, Practical Sampling Techniques for Infrared Analysis, CRC Press, Boca Raton, 1993.
- [126] N.B. Colthup, L.H. Daly, S.E. Wiberley, Introduction to Infrared and Raman Spectroscopy, third ed., Academic Press, San Diego, 1990.